J|A|C|S COMMUNICATIONS

Published on Web 11/03/2006

Gadolinium-Based Hybrid Nanoparticles as a Positive MR Contrast Agent

Hiroki Hifumi,[†] Seiichi Yamaoka,[†] Akihiro Tanimoto,[†] Daniel Citterio,[†] and Koji Suzuki*,[†,‡]

Department of Applied Chemistry, Faculty of Science and Technology, and Department of Diagnostic Radiology, School of Medicine, Keio University, 3-14-1 Hiyoshi, Kohoku-ku, Yokohama 223-8522, Japan, and Core Research for Evolutional Science and Technology (CREST), JST Agency, 4-1-8 Honcho, Kawaguchi, Saitama 332-0012, Japan

Received September 6, 2006; E-mail: suzuki@applc.keio.ac.jp

Magnetic resonance imaging (MRI) is a powerful noninvasive medical diagnostic technique that can differentiate normal tissue from diseased tissue and lesions. An MR image is generated from the nuclear magnetic resonance (NMR) of water protons and the observed contrast essentially depends on the following factors: the water proton density, the longitudinal relaxation time (T_1), and the transverse relaxation time (T_2) of these protons.[1] To increase the contrast in the image, contrast agents (CAs) such as gadolinium (Gd^{3+}) complexes having a high longitudinal relaxivity r_1 and superparamagnetic iron oxide (SPIO) particles having a high transverse relaxivity r_2, are used.[1,2] The relaxivity r is defined as the ratio of the inverse relaxation time and the concentration of the CAs.[3] It is often reported as the parameter r_2/r_1 that gives an indication as to whether CAs are employed as positive or negative CAs. For paramagnetic (but not superparamagnetic) CAs, the r_2/r_1 values become relatively low. When reaching numbers below about 2, brightening is observed in the T_1-weighted images, and thus such CAs are called positive CAs.[4,5]

SPIOs efficiently accumulate in the liver and spleen within minutes of their administration.[6] Furthermore, tumors[7] and atherosclerotic lesions,[8] which cause thrombus formation,[9] with a substantial number of phagocytic cells and/or a significant blood pool may show sufficient uptake of SPIOs that results in a signal decrease of these lesions on T_2-weighted sequences.[7,8] Recently, various nanoparticles were developed relying on a concept applied for drug delivery systems (DDS) using the ability of phagocytosis and the enhanced permeability and retention (EPR) effect.[10] This effect can be applied to tumor tissues, which have unique features such a hypervasculature, defective vascular architecture, and a deficient lymphatic drainage system, resulting in macromolecular nanoparticles and lipids to preferentially accumulate and to retain in the tumor tissue. Therefore, nanoparticles are an attractive form of CAs for diagnostic imaging.

Most existing nanoparticulate CAs, however, are based on iron oxides. Because of their superparamagnetic character, they have high r_2/r_1 values, making them negative CAs. Meanwhile, some nanoparticulate CAs having relatively low r_2/r_1 values have been reported (Table 1), for example, ultrasmall superparamagnetic iron oxides (USPIO) prepared from ferumoxides (Advanced Magnetics, Cambridge, MA),[11] small particulate gadolinium oxides (SPGO),[12] $Gd(BDC)_{1.5}(H_2O)_2$ nanorods (BDC is 1,4-benzendicarboxylate),[13] and GdF_3 nanoparticles.[14] The GdF_3 particles have r_2/r_1 values similar to those of Magnevist (gadolinium-diethylenetriaminepentaacetic acid).[15] The $Gd(BDC)_{1.5}(H_2O)_2$ nanorods have a paramagnetic character; however, they require xanthan gum as a dispersing aid in water. Thus, CAs, which have nanoparticulate shapes, lower r_2/r_1 values, and monodispersibility in water, are desired and may offer a higher signal-to-noise ratio and a better anatomic resolution in T_1-weighted images.[16]

Table 1. Chemical and Physical Properties of Various CAs

CA	composition	r_1 ($mM^{-1}s^{-1}$)	r_2 ($mM^{-1}s^{-1}$)	r_2/r_1
Magnevist	Gd	3.8	4.2	1.1[b]
Resovist	$Fe_2O_3 + Fe_3O_4$	25.4	151.0	5.9[b]
$Gd(BDC)_{1.5}(H_2O)_2$	Gd	35.8	55.6	1.6[c]
USPIO[a]	Fe_2O_3	21.6	44.1	2.0[b]
SPGO	Gd_2O_3	4.8	16.9	3.5[d]
PGP/dextran-K01	$GdPO_4$	13.9	15.0	1.1[b]

[a] USPIO was prepared from ferumoxides. [b] The relaxivity data were measured at 0.47 T. [c] The relaxivity data were measured at 3.0 T containing 0.1% xanthan gum. [d] The relaxivity data were measured at 7.05 T.

To create such CAs, we introduced three concepts for a newly synthesized CA: (1) nanoparticulate structure resulting in characteristic pharmacokinetics,[6−8] (2) paramagnetic properties producing a low r_2/r_1 value for use as a positive CA and thus better contrast for diagnosis,[16] and (3) a particle coating in order to gain monodispersibility in water, retention of water molecules in proximity of the paramagnetic core giving a high relaxivity and toxicity reduction.[17]

We synthesized inorganic−organic hybrid nanoparticles from a suspension of gadolinium(III) nitrate hexahydrate, ammonium hydrogen-phosphate, dextran, and water with an initial pH of 12.5 using a well-known hydrothermal synthesis method.[18] The particles were isolated by centrifugation and washed with distilled water. It was found that the material formed a rodlike shape, consisting of $GdPO_4$ as a core and dextran as a coating material, and had paramagnetic character. A dextran-coating was selected, because of its known high biocompatibility, which is required for in vivo applications.[17] Whereas hydrothermally synthesized materials without a coating generally form agglutinates in water, this dextran coated paramagnetic gadolinium phosphate (PGP/dextran-K01) resulted in monodisperse nanoparticles with an average hydrodynamic diameter of 23.2 ± 7.8 nm (Supporting Information). To confirm the composition and the crystallinity of the materials synthesized in the presence and in the absence of dextran, a powder X-ray diffraction (XRD) analysis was performed (Supporting Information). The XRD patterns of these materials were consistent with $GdPO_4$ in the hydrated form. Transmission electron microscopy (TEM) images of the PGP/dextran-K01 showed that it formed a rodlike shape of uniform size, and the mean particle diameter was about a 20−30 nm in the major axis and about a 6−15 nm in the minor axis (Figure 1). A high-resolution TEM image of this nanorod also exhibited lattice fringes and indicated a high crystallinity. Furthermore, the coating material, dextran, was directly observed with a thickness of less than 5 nm under the condition of a 120 kV accelerating voltage. The existence and the identification of dextran

[†] Keio University.
[‡] JST-CREST.

10.1021/ja066442d CCC: $33.50

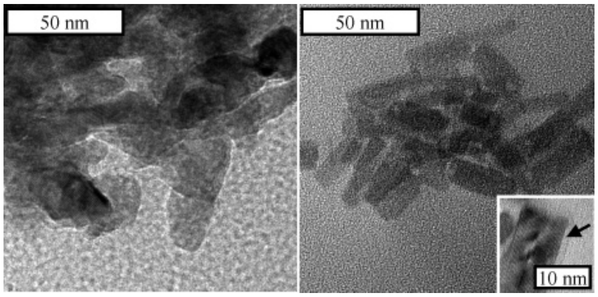

Figure 1. TEM images of $GdPO_4$ particles without (left) and with (right, PGP/dextran-K01) the dextran coating. (The arrow in the right picture indicates the dextran coating material.)

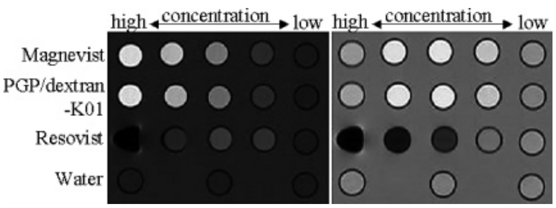

Figure 2. T_1-weighted (left) and T_2-weighted (right) MR images of various concentrations of CAs and water. First row: Magnevist (from the left) 5.0, 1.0, 0.5, 0.1, 0.01 mM. Second row: PGP/dextran-K01 (from the left) 2.2, 1.1, 0.5, 0.2, 0.04 mM of Gd^{3+}. Third row: Resovist (from the left) 5.0, 1.0, 0.5, 0.1, 0.01 mM of Fe^{3+}. Fourth row: water.

was also confirmed using Fourier transform infrared (FTIR) spectroscopy showing peaks characteristic of dextran around 3400 cm^{-1}, 2950−2850 cm^{-1}, 1156 cm^{-1}, and 1013 cm^{-1} corresponding to the O−H, the C−H, the antisymmetrical C−O−C, and the C−O stretching vibrations, respectively (Supporting Information). Although the hydrothermal synthesis method applied here has previously been used especially for the preparation of metal oxides for ceramics and optical materials, PGP/dextran-K01 is the first material that has a gadolinium phosphate core and a dextran coating resulting in stable monodispersed particles in water.

To estimate the r_2/r_1 value of PGP/dextran-K01, relaxivity data were obtained from clear dispersions of PGP/dextran-K01 in water. These showed high r_1 and r_2 values of 13.9 and 15.0 s^{-1} per mM of Gd^{3+}, respectively, and thus 1.1 as the r_2/r_1 value (Table 1 and Supporting Information), indicating that PGP/dextran-K01 is a paramagnetic material. The paramagnetic character is also supported by the result of a SQUID measurement (Supporting Information). This low r_2/r_1 value has a significant advantage for its use as a positive CA.[5,16]

Figure 2 shows the MR images of solutions of various PGP/dextran-K01 concentrations as well as the present clinically used positive CA Magnevist and the negative CA Resovist as a reference.[15,19] The T_1-weighted images of PGP/dextran-K01 gradually become brighter with higher concentrations analogous to Magnevist. On the contrary, the images using Resovist become darker with higher concentrations in the T_2-weighted images, whereas those obtained with PGP/dextran-K01 show little darkening with increasing concentration, as is the case for Magnevist. These results agree with the relaxivity data indicating that PGP/dextran-K01 has a significantly low r_2/r_1 value and thus functions as a positive CA.

In vivo toxicity studies have not yet been performed. However, no significant leaching of Gd^{3+} from the nanoparticles has been observed in aqueous solution (Supporting Information).

In conclusion, we have developed and succeeded in synthesizing a dextran-coated $GdPO_4$ nanoparticle using a hydrothermal synthesis method in the simultaneous presence of dextran. PGP/dextran-K01 has monodispersibility in water and a significantly low r_2/r_1 value and therefore, may be a useful substitute for nanoparticulate negative CAs based on iron oxides. Therefore, a diagnostic alternative for MRI could become available, and the diagnostic accuracy and ease-of-use may be improved in the fields of imaging tumors, atherosclerotic lesions, the lymphatic system, and others, as well as in MR angiography (MRA).[5] The next step in this investigation is to vary the thickness of the dextran coating to attempt to optimize the relaxivity. Finally, the application for detection of in vivo lesions will be addressed.

Acknowledgment. This work was supported by JSPS Research Fellowship for Young Scientists and Grant-in-Aid for the 21st Century COE program “KEIO LCC” from the Ministry of Education, Culture, Sports, Science, and Technology, Japan.

Supporting Information Available: Preparative procedures and analytical data for PGP/dextran-K01. This material is available free of charge via the Internet at http://pubs.acs.org.

References

(1) (a) Lauffer, R. B. *Chem. Rev.* **1987**, *87*, 901. (b) Caravan, P.; Ellison, J. J.; McMurry, T. J.; Lauffer, R. B. *Chem. Rev.* **1999**, *99*, 2293.
(2) (a) Fahlvik, A. K.; Klaveness, J.; Stark, D. D. *J. Magn. Reson. Imaging* **1993**, *3*, 187. (b) Tiefenauer, L. X.; Tschirky, A.; Kuhne, G.; Andres, R. Y. *Magn. Reson. Imaging* **1996**, *14*, 391.
(3) See Supporting Information.
(4) (a) Josephson, L.; Lewis, J.; Jacobs, P.; Hahn, P. F.; Stark, D. D. *Magn. Reson. Imaging* **1988**, *6*, 647. (b) Pouliquen, D.; Perroud, H.; Calza, F.; Jallet, P.; Le Jeune, J. J. *Magn. Reson. Med.* **1992**, *24*, 75.
(5) (a) Koenig, S. H.; Kellar, K. E. *Magn. Reson. Med.* **1995**, *34*, 227. (b) Kellar, K. E.; Fujii, D. K.; Gunther, W. H. H.; Briley-Saebo, K.; Spiller, M.; Koenig, S. H. *Magn. Reson. Mater. Phys.* **1999**, *8*, 207.
(6) (a) Hamm, B.; Staks, T.; Taupitz, M.; Maibauer, R.; Speidel, A.; Huppertz, A.; Frenzel, T.; Lawaczeck, R.; Wolf, K. J.; Lange, L. *J. Magn. Reson. Imaging* **1994**, *4*, 659. (b) McLachlan, S. J.; Morris, M. R.; Lucas, M. A.; Fisco, R. A.; Eakins, M. N.; Fowler, D. R.; Scheetz, R. B.; Olukotun, A. Y. *J. Magn. Reson. Imaging* **1994**, *4*, 301. (c) Weissleder, R.; Stark, D. D.; Engelstad, B. L.; Bacon, B. R.; Compton, C. C.; White, D. L.; Jacobs, P.; Lewis, J. *Am. J. Roentgenol.* **1989**, *152*, 167.
(7) (a) Weissleder, R. *Radiology* **1994**, *193*, 593. (2) Hahn, P. F.; Stark, D. D.; Elizondo, G.; Weissleder, R.; Saini, S.; Ferrucci, J. T. *Radiology* **1990**, *174*, 361.
(8) (a) Ross, R. *Nature* **1993**, *362*, 801. (b) Schmitz, S. A.; Coupland, S. E.; Gust, R.; Winterhalter, S.; Wagner, S.; Kresse, M.; Semmler, W.; Wolf, K. J. *Invest. Radiol.* **2000**, *35*, 460.
(9) (a) Davies, M. J. *Circulation* **1996**, *94*, 2013. (b) Falk, E.; Shah, P. K.; Fuster, V. *Circulation* **1995**, *92*, 657. (c) Lusis, A. J. *Nature* **2000**, *407*, 233.
(10) (a) Matsumura, Y.; Maeda, H. *Cancer Res.* **1986**, *46*, 6387. (b) Maeda, H.; Matsumura, Y. *Drug Carrier Syst.* **1989**, *6*, 193. (c) Muggia, F. *Clin. Cancer Res.* **1999**, *5*, 7. (d) Vasey, P. A.; Kaye, S. B.; Morrison, R.; Twelves, C.; Wilson, P.; Duncan, R.; Thomson, A. H.; Murray, L. S.; Hilditch, T. E.; Murray, T.; Burtles, S.; Fraier, D.; Frigerio, E.; Cassidy, J. *Clin. Cancer Res.* **1999**, *5*, 83.
(11) (a) Groman, E. V.; Josephson, L.; Lewis, J. M. U.S. Patent 4,827,945, 1989. (b) Weissleder, R.; Elizondo, G.; Wittenberg, J.; Rabito, C. A.; Bengele, H. H.; Josephson, L. *Radiology* **1990**, *175*, 489.
(12) (a) McDonald, M. A.; Watkin, K. L. *Acad. Radiol.* **2006**, *13*, 421. (b) McDonald, M. A.; Watkin, K. L. *Invest. Radiol.* **2003**, *38*, 305.
(13) Rieter, W. J.; Taylor, K. M. L.; An, H.; Lin, W.; Lin, W. *J. Am. Chem. Soc.* **2006**, *128*, 9024.
(14) Evanics, F.; Diamente, P. R.; Van Veggel, F. C. J. M.; Stanisz, G. J.; Prosser, R. S. *Chem. Mater.* **2006**, *18*, 2499.
(15) Mikawa, M.; Kato, H.; Okumura, M.; Narazaki, M.; Kanazawa, Y.; Miwa, N.; Shinohara, H. *Bioconjugate Chem.* **2001**, *12*, 510.
(16) (a)Harika, L.; Weissleder, R.; Poss, K.; Zimmer, C.; Papisov, M. I.; Brady, T. J. *Magn. Reson. Med.* **1995**, *33*, 88. (b)Harika, L.; Weissleder, R.; Poss, K.; Papisov, M. I. *Radiology* **1996**, *198*, 365. (c)Misselwitz, B.; Sachse, A. *Acta Radiol. Suppl.* **1997**, *412*, 51.
(17) Shen, T.; Weissleder, R.; Papisov, M.; Bogdanov, A., Jr.; Brady, T. J. *Magn. Reson. Med.* **1993**, *29*, 599.
(18) Laudise, R. A. *Prog. Inorg. Chem.* **1962**, *3*, 1.
(19) (a) Reimer, P.; Marx, C.; Rummeny, E. J.; Muller, M.; Lentschig, M.; Balzer, T.; Dietl, K. H.; Sulkowski, U.; Berns, T.; Shamsi, K.; Peters, P. E. *J. Magn. Reson. Imaging* **1997**, *7*, 945. (b) Tanimoto, A.; Kuribayashi, S. *Eur. J. Radiol.* **2006**, *58*, 200.

JA066442D